Title
Cooperation within von Willebrand factors enhances adsorption mechanism

Journal
Journal of The Royal Society Interface, 12(109)

ISSN
1742-5689

Authors
Heidari, Maziar
Mehrbod, Mehrdad
Ejtehadi, Mohammad Reza
et al.

Publication Date
2015-08-01

DOI
10.1098/rsif.2015.0334

Peer reviewed

INTERFACE

rsif.royalsocietypublishing.org

Research

Cite this article: Heidari M, Mehrbod M, Ejtehadi MR, Mofrad MRK. 2015 Cooperation within von Willebrand factors enhances adsorption mechanism. *J. R. Soc. Interface* **12**: 20150334.
http://dx.doi.org/10.1098/rsif.2015.0334

Received: 15 April 2015
Accepted: 23 June 2015

Subject Areas:
biomechanics, bioengineering, biophysics

Keywords:
von Willebrand factor, cooperativity, coarse-grained modelling, adsorption mechanism

Author for correspondence:
Mohammad R. K. Mofrad
e-mail: mofrad@berkeley.edu

†Present address: Max Planck Institute for Polymer Research, Ackermannweg 10, Mainz 55128, Germany.

Electronic supplementary material is available at http://dx.doi.org/10.1098/rsif.2015.0334 or via http://rsif.royalsocietypublishing.org.

THE ROYAL SOCIETY PUBLISHING

Cooperation within von Willebrand factors enhances adsorption mechanism

Maziar Heidari[1,†], Mehrdad Mehrbod[1], Mohammad Reza Ejtehadi[2] and Mohammad R. K. Mofrad[1]

[1]Molecular Cell Biomechanics Laboratory, Departments of Bioengineering and Mechanical Engineering, University of California, Berkeley, CA 94720, USA
[2]Department of Physics and Center of Excellence in Complex Systems and Condensed Matter, Sharif University of Technology, Tehran, Iran

von Willebrand factor (VWF) is a naturally collapsed protein that participates in primary haemostasis and coagulation events. The clotting process is triggered by the adsorption and conformational changes of the plasma VWFs localized to the collagen fibres found near the site of injury. We develop coarse-grained models to simulate the adsorption dynamics of VWF flowing near the adhesive collagen fibres at different shear rates and investigate the effect of factors such as interaction and cooperativity of VWFs on the success of adsorption events. The adsorption probability of a flowing VWF confined to the receptor field is enhanced when it encounters an adhered VWF in proximity to the collagen receptors. This enhancement is observed within a wide range of shear rates and is mostly controlled by the attractive van der Waals interactions rather than the hydrodynamic interactions among VWF monomers. The cooperativity between the VWFs acts as an effective mechanism for enhancing VWF adsorption to the collagen fibres. Additionally, this implies that the adsorption of such molecules is nonlinearly dependent on the density of flowing VWFs. These findings are important for studies of primary haemostasis as well as general adsorption dynamics processes in polymer physics.

1. Introduction

von Willebrand factor (VWF) is a large multimeric glycoprotein that plays a vital role in coagulation and haemostasis [1,2]. Upon rupture of vascular walls, the plasma VWFs, whose monomers contain the modular domains of D′-D3-A1-A2-A3-D4-B1-B2-B3-C1-C2-CK [2], adhere to the subendothelial collagen fibres I and II via their A3 binding domains. The molecular structure of VWF is then stretched out, consequently leading to exposure of their A1 binding sites to the platelets' GPIbα receptors as shown in figure 1 [1–6]. The coagulation process further involves a direct attachment of platelet receptors to collagen fibres. However, it has been observed that such platelet–collagen interactions cannot withstand the hydrodynamic stresses found in shear rates above 1500 s^{-1} [1]. Hence, the success of thrombosis relies on the presence of VWF such that, on the one hand, its A3 binding sites interact with the collagen fibres and, on the other hand, its A1 domains interact with the platelets' GPIbα receptors (figure 1). This relies on adsorption of VWF through interactions of VWF's A3 binding sites to the collagen fibres and afterward, the integrin–RGD interactions between the VWF's A1 domains and the platelet's GPIbα receptors [1]. In the proximity of the vessel wall surface, VWF experiences a hydrodynamic lift force that keeps it away from the receptor field [7]. However, this wall-repulsive force could be overcome by hydrodynamic and attractive interactions between VWF molecules such that the adsorbed VWF assists the flowing VWF to approach the receptor field. The interplay between the hydrodynamic lift force and the attractive intermolecular forces plays an

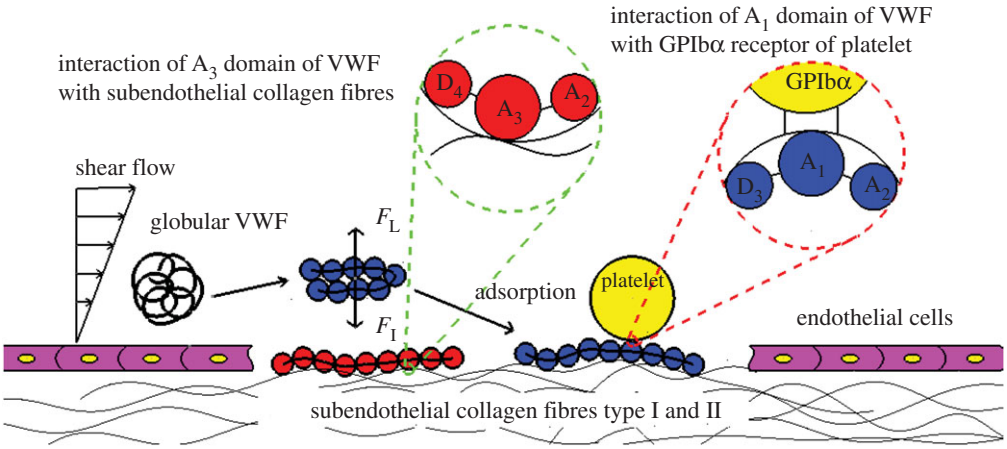

Figure 1. The adsorption mechanism in primary haemostasis in the case of rupture at vessel walls demonstrated schematically. The initially adsorbed and plasma VWF are shown in red and blue polymer chain, respectively. Each monomer (as shown with circle) of VWF contains modular domains of D′-D3-A1-A2-A3-D4-B1-B2-B3-C1-C2-CK. The specific interaction of VWF domains with subendothelial collagen fibres type I and II as well as platelets are shown in the zoomed circles. The plasma VWF experiences the hydrodynamic lift force (F_L) and the attractive force (F_I) when it passes over the adsorbed VWF. (Online version in colour.)

important role in the adsorption process of such biopolymers and the subsequent coagulation process.

The dynamics of VWF and self-associated polymers in the flow has received great attention in recent years [8–14]. It has been observed that the stretching length of a single molecule of VWF, which naturally has a globular conformation, increases drastically when exposed to shear rates greater than 5000 s^{-1} [15]. Such a transition in the structure of VWF from the globular to the stretched conformations enables the exposure of more binding sites for the collagen receptors, increasing VWF adsorption likelihood under a high shear rate [15,16]. Beside this complex behaviour at the single-molecule level, VWFs exhibit interesting cooperative effects through formation of reversible structures in colloidal suspensions when the shear rate varies [8,17]. Furthermore, such a cooperation, which is originated from the interactions as well as the self-association capabilities of the VWF monomers, has been observed in the concentrated system of VWFs under high shear rates by the creation of a web-like network on collagen-coated substrates [9,15].

Adhesion dynamics of a single VWF molecule on a collagen surface have been recently studied using computational models that simulated the interaction of the A3-domains of VWF with collagen receptors [16]. In this study, we develop models of VWF incorporating specific interactions among monomers of VWF and the collagen receptors, investigating the adsorption dynamics of a flowing VWF in proximity to an adhered VWF molecule. The cooperation between VWFs is shown to increase the adsorption probability.

Our results are significant because we show unprecedentedly that during the early stages of primary homeostasis, the adsorbed VWF molecule cooperates with the marginated flowing VWF to improve its adsorption probability. This cooperation is observed in a wide range of shear rates. Interestingly, in high shear rate regimes, in contrast to the hydrodynamic lift force keeping the flowing VWF away from the adsorbed VWF molecules, the stretched conformations of both molecules, i.e. the VWF adsorbed to the surface and the one flowing, increases the attractive intermolecular interactions and accordingly augments the cooperativity among the VWF molecules to enhance the adsorption process.

2. Material and methods

A coarse-grained model is developed for the VWF using a multi-particle collision dynamics (MPCD) approach with fluid modelled as a system of particles. The dynamics of particles is evolved locally and synchronously with continuous velocities at discrete time steps [18]. This particle-based method takes the thermal fluctuations as well as the hydrodynamic interactions into account for polymer systems [19–21]. The MPCD consists of N_s particles with mass m_s each, which are confined in a simulation box edge dimensions as $L_x/a = 60$, $L_y/a = 20$ and $L_z/a = 20$, where a denotes the size of the cubic MPCD lattices. The position and velocity of the MPCD particles are evolved in two sequential steps: streaming and collision [18].

In the streaming step, the positions of the solvent particles r_i^s are integrated according to $r_i^s(t + \Delta t_{CD}) = r_i^s(t) + v_i^s(t)\Delta t_{CD}$, where $v_i^s(t)$ is the particle velocity and Δt_{CD} is the time interval between two successive collisions. In the collision step, the particles are sorted into lattices of size a and the particle velocities $v_i^s(t)$ that share a lattice are updated as $v_i^{s,new}(t) = v_{cm}^s(t) + \Omega_{\pi/2}(v_i^s(t) - v_{cm}^s)$, where the velocity of the lattice centre of mass, v_{cm}^s, is calculated by averaging the velocity of particles that are included in that lattice. The rotational operator $\Omega_{\pi/2}(x)$ rotates vector x by angle $\pi/2$ about a randomly chosen axis in each lattice.

An average lattice density of $\rho = 10\ m_s/a^3$ and a MPCD time-step $\Delta t_{CD} = 0.025$ were used corresponding to a solvent viscosity of $\eta_0 = 20.1\ \sqrt{m_s k_B T/a^2}$ [20]. To preserve the Galilean invariance, the random shift method is applied before each collision step [22]. Our simulations were carried out using NVT ensembles with a velocity-scaling thermostat used to enforce isothermal processes. The boundary conditions along the x- and y-directions of the simulation box were periodic and the shear flow was applied along the x-direction. The wall at $z = 0$ was fixed while a constant velocity boundary condition was applied at the wall at $z = L_z$ corresponding to the assigned shear rates. To implement the zero velocity at $z = 0$, the virtual-particles method as well as bounce-back boundary condition are adopted [21].

The VWF is modelled as a coarse-grained polymer using monomers of radius $a_p = 0.25a$ with potentials $U_p = U_s + U_{lj} + U_r + U_w$

(see below for a detailed description), defining the interaction among monomers [16]. The harmonic potential, which preserves the connectivity among monomers, is given by $U_s = \kappa/2 \sum_{i=1}^{N_p-1} (r_{i+1,i} - 2a_p)^2$. The relative distance of the neighbouring monomers is denoted by $r_{i+1,i}$ while $\kappa = 200 k_B T/a_p^2$ is the spring stiffness [16,23]. The pairs of the monomers also interact through the Lennard–Jones potential $U_{lj} = \epsilon \sum_{ij} [(2a_p/r_{ij})^{12} - 2(2a_p/r_{ij})^6]$, where ϵ corresponds to the depth of the potential well and r_{ij} is the distance between monomers i and j. It has been shown that for the case of $\epsilon = 2.0 k_B T$, the polymer forms a self-associated globular structure similar to the relaxed globular conformation of the VWF [16,23]. In this model, N_r beads, resembling the subendothelial collagen receptors, are uniformly distributed on the surface located at $z = a/2$ resembling a receptor density of ϕ. The specific interactions between collagen beads and A3 domains of the VWF monomers are simulated by the Bell mechanism [8,16,24]. According to this mechanism, when a monomer of VWF is located within the reaction distance of the collagen bead ($R_{reac} = a_p$), a bond between the monomer and its corresponding collagen bead is formed with probability of $P_B = \exp(-U_B/k_B T)$, where U_B is the binding energy and it is assumed that the VWF monomers can solely form one bond with each collagen bead. This bond is modelled by a harmonic spring with potential energy of $U_r = \kappa/2(r_{i,p} - r_{j,r})^2$ [11,16]. The position of the ith VWF monomer and the jth collagen receptor are denoted by $r_{i,p}$ and $r_{j,r}$, respectively. While attached, VWF could be dissociated with the probability of $P_{UB} = \exp(-U_{UB}/k_B T)$, where U_{UB} is the unbinding energy [16]. The difference between binding and unbinding energies is named as bonding energy and denoted by $\Delta E_0 = U_B - U_{UB}$. To allow an unbound ligand to have sufficient time to diffuse away from a receptor, the binding and unbinding attempts are carried out every $\tau_0 = 100$ MPC steps. To confine VWFs within a specific height with respect to the receptor field, a repulsive wall with the potential of U_w is included such that it is analogous to the repulsive part of U_{lj}. The elevation of this repulsive wall is such that it does not affect the initial height of the globule centre of mass (ΔZ^0_{CM}) with respect to the receptive field. The receptor field and repulsive wall are illustrated in figure 2 with grey beads and a purple dashed line, respectively. The position and velocity of the monomers are integrated using the velocity-Verlet algorithm with time steps $\Delta t_{MD} = \Delta t_{CD}/20$. The monomers interact with solvent particles by participating in collision steps [19]. The characteristic timescale, defined by the monomer diffusion time, is calculated by $\tau = 6\pi\eta a_p^3/k_B T$. In the first step, the VWF is embedded in the bulk flow where neither the receptor field nor the repulsive wall is present. The first 5000 MPC steps are allocated for the relaxation and the shear flow is induced afterward. The extension length of VWF along the x-axis is denoted by R_s and its rescaled averaged value $R_s/2N_p a_p$ against normalized shear rates $\dot{\gamma}\tau$ is shown with the filled diamonds in figure 3. By calculating the variance of the squared VWF extension (the results are not shown), the transitional shear rate becomes $\dot{\gamma}_c \tau = 10$ which matches well with the formerly reported data [23].

The VWF is initially kept in the proximity of the receptor field, where $N_r = 4800$ receptors are placed with the density of $\varphi_r = 2/a^2$. After 5000 MPC steps of relaxation, the shear flow is introduced. The fraction of time in which the number of adhered monomers becomes larger than 10 is denoted by $T_{Nb>10}$ [16]. This is shown in figure 3 for different values of shear rates as well as different values of ΔE_0. In this figure, the unbinding energy is kept constant so that the unbinding time, which is determined by $\tau_{UB} = \tau_0 \exp(U_{UB}/k_B T)$, matches well for all cases. In the case of $\Delta E_0 = -1.0 k_B T$, the transitional behaviour of VWF adhesion dynamics (figure 3, triangle symbols) coincides well with that of the stretching dynamics (diamond symbols) of VWF. This bonding energy also falls within the previously reported energy range, which explains the VWF's adhesion behaviour [16]. Thus, we consider $\Delta E_0 = -1.0 k_B T$ as the bonding energy and $\varphi_r = 2/a^2$ as the receptor density.

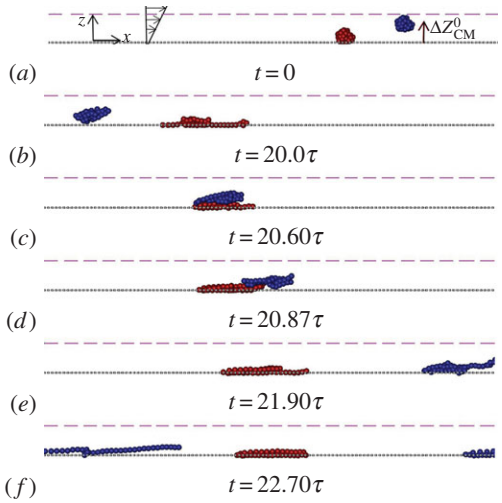

Figure 2. (*a*) The initial condition for two globular VWFs is shown where the adhered VWF (red) is located near the receptor field and the centre of mass of the flowing VWF (blue) is ΔZ^0_{CM} above the receptor surface. The collagen receptors and repulsive wall are illustrated by the grey dots and a purple dashed line, respectively. (*b–f*) The snapshot series of simulation for the case in which the flowing VWF is initially located $\Delta Z^0_{CM} = 10\ a_p$ above the receptor field and the rescaled shear rate is $\dot{\gamma}\tau = 16$. The flowing VWF becomes adhered at $t = 21.9\tau$. (Online version in colour.)

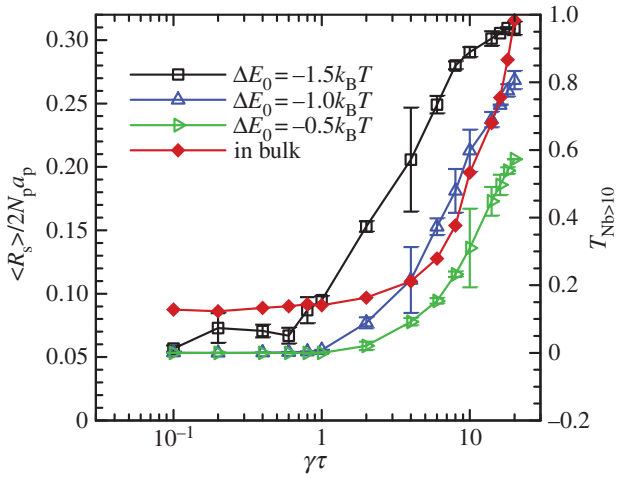

Figure 3. The rescaled extension $R_s/2N_p a_p$ of VWF as a function of normalized shear rate $\dot{\gamma}\tau$ is shown in filled diamonds. The fraction of time in which VWF has more than 10 monomers attached ($T_{Nb>10}$) for different values of bonding energies $\Delta E_0 = -1.5 k_B T$ (squares), $\Delta E_0 = -1.0 k_B T$ (triangles), $\Delta E_0 = -1.0 k_B T$ (filled triangles) are shown as well. The error bar is calculated over the simulation time of 200τ. (Online version in colour.)

3. Results and discussions

We used our coarse-grained model of the VWF polymers together with the MPCD approach for the fluid in order to examine whether and how pairwise interactions among the monomers of VWFs affect the adsorption mechanism of a flowing VWF. The monomers of the first VWF were initially located within the reaction radius of the receptors such that the VWF associates with the collagen receptors. The distance

of the second (flowing) VWF centre of mass with respect to the receptor surface is ΔZ^0_{CM} (figure 2). Additionally, the initial y components of both VWFs are set to $L_y/2$. A repulsive wall was also placed at $\Delta Z^0_{CM} + \Delta Z$ (where ΔZ is calculated by the summation over the radius of the globule and the cut-off radius of the repulsive wall). The implementation of such repulsive wall determines the density of VWF molecules near the collagen fibres. By changing the cut-off radius of the repulsive wall, we ensured that this parameter does not affect the VWF conformation and dynamics results (data not presented). Both VWF molecules were relaxed before the shear flow is introduced for $T = 100\tau$. Once the shear was applied, the VWF located near the receptors adhered to the surface and then stretched out while the other VWF molecules moved along the x-axis. After passing over the adhered VWF several times, the flowing VWF reduced its height and finally its monomers fell into the reaction radius of the receptors before it was adsorbed. The snapshot series of the adsorption procedure when the initial height of the flowing VWF centre of mass is $\Delta Z^0_{CM} = 10a_p$ and the shear rate is $\dot{\gamma}\tau = 16$ is shown in figure 3. Another simulation was implemented with an identical set-up except with only one flowing VWF in the absence of an adhered VWF. The simulations were repeated for six sets of five trials and in each set, the adsorption probability was calculated as the fraction of times in which the flowing VWF was adsorbed relative to the total number of trials. The adsorption probability is presented in figure 4*a*,*b* for different initial heights of the flowing VWF as well as different shear rates when there was only one flowing VWF ($n_{VWF} = 1$) or with one adhered VWF and another flowing VWF ($n_{VWF} = 2$). The simulations of the system in which the shear rate is $\dot{\gamma}\tau = 16$ are shown in the electronic supplementary material, movie. Adhered and flowing VWFs had roughly globular structures for shear rates smaller than $\dot{\gamma}\tau = 8$ and their structures became stretched when they experienced a higher shear rate. The flowing VWF completely adhered to the surface when $\Delta Z^0_{CM} = 6a_p$ and $n_{VWF} = 2$, however, this probability decreased for higher shear rates with only one flowing VWF ($n_{VWF} = 1$). For the case of $\Delta Z^0_{CM} = 8a_p$ and $n_{VWF} = 2$, the adsorption probability of the flowing VWF was remarkably higher than that in the $n_{VWF} = 1$ scenario and this behaviour was observed within a wide range of shear rates. The same adsorption trend was also observed when $\Delta Z^0_{CM} = 10a_p$, however, the adsorption probability for both cases with $n_{VWF} = 1$ and $n_{VWF} = 2$ decreased as the distance between the flowing and adhered VWFs increased. The hydrodynamic as well as van der Waals interactions are two possible causes behind the enhancement of the adsorption probability. To isolate the effects of each interaction and differentiate their impact on the adsorption behaviour of the flowing VWF, the attraction part of the Lennard–Jones potential between the monomers of VWFs was switched off, leaving only the repulsive potential. Hence, interactions among the VWF monomers were only hydrodynamic and steric. The hydrodynamic interaction between the flowing VWF and the adhered one is important because the adhered VWF is not totally fixed at the collagen surface and it may change the flow velocity field through its conformational changes caused by the dynamics of attachment and detachment of its beads near the collagen receptors. The adsorption probability of the flowing VWF for the case of $\Delta Z^0_{CM} = 8a_p$ is shown in figure 4*b* where only the hydrodynamic interactions among the VWF monomers are present. The absence of attracting interactions among the VWF monomers approximately resulted in similar trends found in the case without adhered VWFs. These simulations suggest that hydrodynamic interactions are not sufficient to enhance the adsorption mechanism, but they do not reject their necessity in the adsorption events. Nevertheless, the attractive interaction plays a major role in adsorbing flowing VWFs such that the presence of an adhered VWF perturbs the spatial distribution of the flowing VWF monomers along the z-direction, and forces them to approach the receptor field and, ultimately, increases the probability of falling within the reaction region of the receptors. The probability distribution function (PDF) of positions of flowing VWF monomers along the z-direction for two initial heights $\Delta Z^0_{CM} = 8a_p$ (square symbols) and $\Delta Z^0_{CM} = 10a_p$ (triangle symbols) are shown in figure 4*c*. In these simulations, the adhesion ability of the flowing VWF monomers was switched off such that they could not form bonds with the receptors. The presence of an adhered VWF caused the maxima of the PDFs to shift towards the lower heights and this is remarkable for the case in which the initial height of the flowing VWF is $\Delta Z^0_{CM} = 8a_p$.

It should be noted that the adsorption probabilities in figure 4*a*,*b* are calculated over the cases wherein the flowing VWF approaches the surface and at least one of its monomers attaches to the collagen receptors. To analyse the adhesion dynamics of the flowing VWF to the collagen receptors after it is adsorbed on the surface, we calculate the adhesion rate and the height of the centre of mass of the flowing VWF for the cases in which the flowing VWF approaches the collagen receptors and are adsorbed on the surface. As shown in figure 5, the adsorbed flowing VWF is extended and while approaching the collagen surface as the shear rate increases. Concurrently, the adhesion rates of adsorbed flowing VWF increases and the trend is analogous to the cases where the VWF is initially adsorbed on the surface (figure 3) and earlier experimental reports [15,16].

4. Conclusion

The adsorption dynamics of VWF multimeric glycoproteins, which are the triggering cause of primary haemostasis, were studied here using coarse-grained models. Our results suggest that when a VWF molecule is flowing in proximity to a collagen receptor field, its monomers, which includes the A3 domains, may fall within the reaction region of the collagen receptors and form bonds. This behaviour is caused by the conformational changes and instabilities exhibited in the VWF molecule under the influence of hydrodynamic shear forces as well as thermal fluctuations. However, when a flowing VWF glycoprotein is passing over another VWF that is adhered to the collagen receptor field, it approaches the surface and its adsorption is enhanced due primarily to attractive interactions rather than hydrodynamic interactions among the VWF monomers. Given $\eta = 10^{-3}$ Pa s as the viscosity of water and $a_p = 70$ nm as the radius of the VWF monomer [23,25], such enhancement in the adsorptions occurs within the wide range of shear rate $\dot{\gamma} \approx 1300 - 12\,000\ s^{-1}$, in which the flowing VWF has either a roughly globular or extended conformation [15].

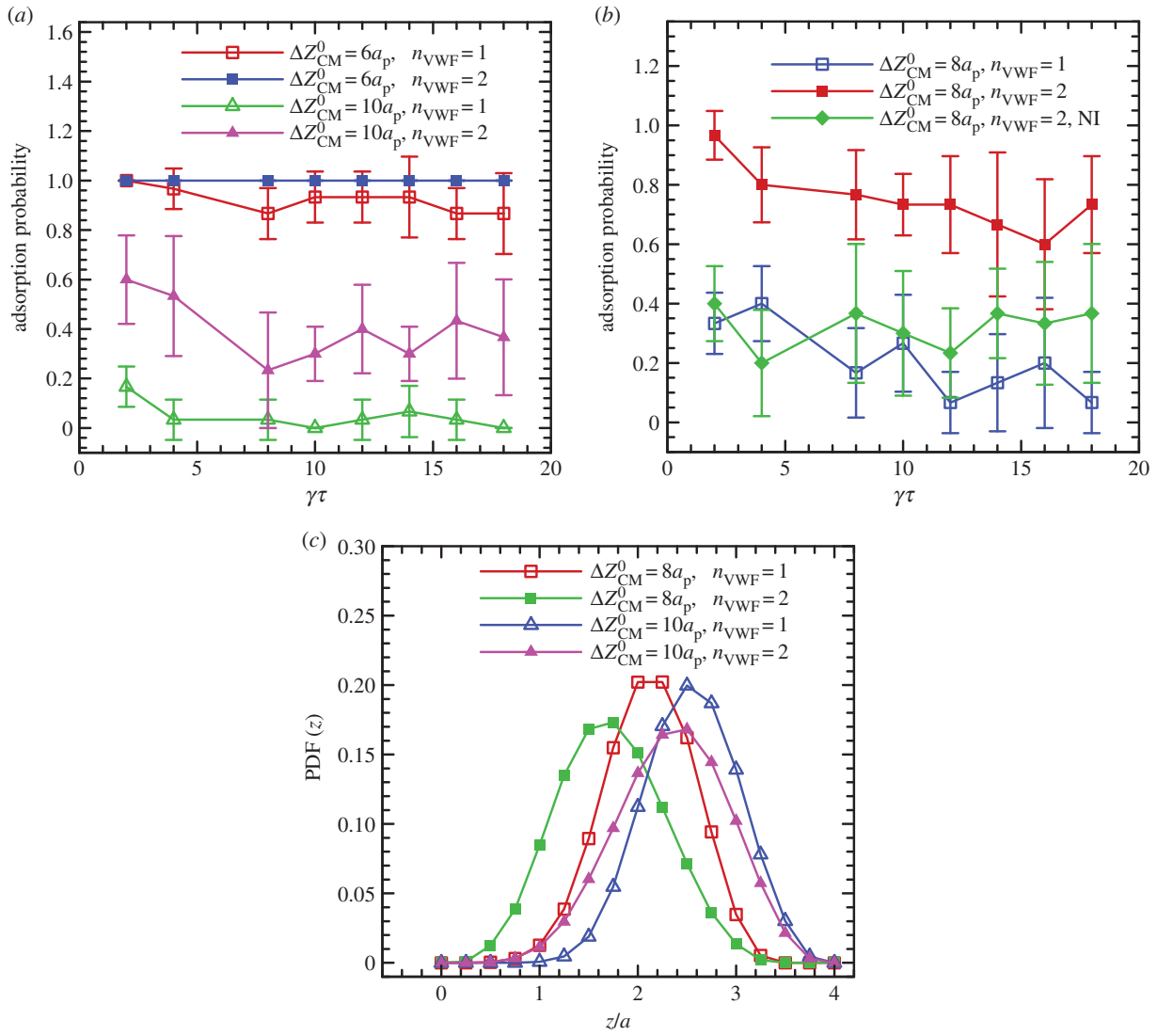

Figure 4. The adhesion probability of the flowing VWFs initially located at (*a*) $\Delta Z^0_{CM} = 6a_p$ and $\Delta Z^0_{CM} = 10a_p$, and (*b*) $\Delta Z^0_{CM} = 8a_p$ above the receptor fields. (*c*) The PDF of the flowing VWF's monomers along the *z*-direction for two initial heights $\Delta Z^0_{CM} = 8a_p$ (squares) and $\Delta Z^0_{CM} = 10a_p$ (triangles). In all cases, the open and filled symbols represent the adhesion probability as well as PDFs of those flowing VWFs that are not accompanied by the adhered VWF ($n_{VWF} = 1$) and those in which the adhered VWFs are present ($n_{VWF} = 2$). The error bars in section (*c*) are smaller than the size of the symbols. (Online version in colour.)

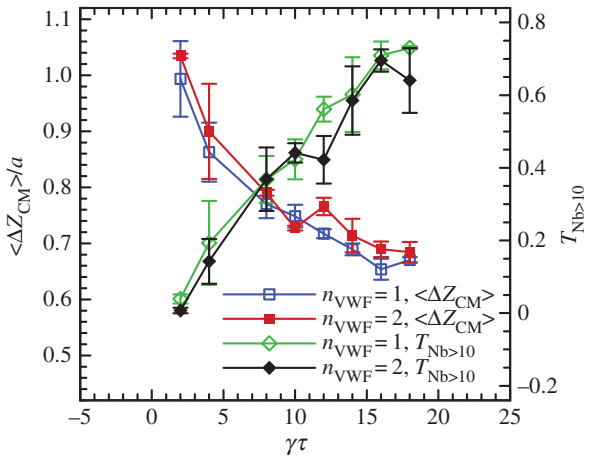

Figure 5. The averaged height of the centre of mass of the flowing VWF (ΔZ_{CM}) and its corresponding adhesion rate ($T_{Nb>10}$) to the collagen receptors as a function of rescaled shear rates ($\dot{\gamma}\tau$) are shown in squares and diamonds, respectively. The results are taken from the cases in which the flowing VWF approaches the collagen receptors and is adsorbed on the surface. The white and filled symbols represent the cases in which there is one ($n_{VWF} = 1$) or two VWFs ($n_{VWF} = 2$) in the system, respectively. (Online version in colour.)

The hydrodynamic lift force exerted on the monomers has an increasing functionality with respect to the shear rate and the extended length of the polymer (L), $f_L = g(\dot{\gamma}, L^4)$ [16]. Hence, the cooperation within VWFs should increase in high shear rate regimes to overcome the hydrodynamic lift force, as observed in our simulations, likely because in a high shear rate both the flowing and adhered VWFs have extended conformations, increasing their attractive interaction. Additionally, our results reveal that in addition to the shear stress that triggers the adsorption of VWF [16], the immobilized adsorbed VWF boosts the adsorption of flowing VWFs nearby. The adsorption dependency of flowing VWFs on the presence of another adsorbed VWF implies the nonlinear dependency of adsorbed VWFs on the density of flowing VWFs. Accordingly, the adsorption success rate increases drastically as the number of adsorbed VWFs on the collagen surface increases. For a height of 400 nm or less, the cooperativity between VWFs leads to adsorption of all flowing VWFs. Hence, the adsorption process is definitely accomplished if there exists a corresponding biological mechanism that forces VWFs to be marginated within this range. It has recently been shown that the colloidal suspension, which

can correspond to the other blood components such as red blood cells, could affect the spatial distributions of the globule polymers [11]. The observed cooperation within VWF molecules adhered on the collagen surface could also be investigated in a system where a larger number of VWF molecules are included. Recent research and experiments have elaborated on the collective motion as well as self-assembly of globular polymers and VWFs when they are either located in the bulk flow or adsorbed on an adhesive surface [4–6,8,9,11,17,26]. Our results could potentially be important for studies of adsorption dynamics of polymer physics as well as the current mathematical and coarse-grained models [3] used to analyse primary haemostasis and coagulation processes.

Data accessibility. The article's supporting data can be accessed via our laboratory's website (http://biomechanics.berkeley.edu). The supplementary movie can be found at http://biomechanics.berkeley.edu/wp-content/uploads/2015/07/VWF_Movie1.avi.

Authors' contributions. M.H., M.R.E. and M.R.K.M. conceived and designed the experiments. M.H. performed the experiments. M.H., M.M., M.R.E. and M.R.K.M. analysed the data. M.R.E. and M.R.K.M. contributed reagents/materials/analysis tools. M.H., M.M., M.R.E. and M.R.K.M. wrote the paper.

Competing interests. The authors have no competing interests.

Funding. Financial support through a National Science Foundation CAREER award CBET-0955291 (M.R.K.M.) is gratefully acknowledged.

Acknowledgements. M.H. thanks Math. Computing Center of Institute for Research in Fundamental Sciences (IPM) where a part of the computation was carried out.

References

1. Reininger AJ. 2008 Function of von Willebrand factor in haemostasis and thrombosis. *Haemophilia* **14**, 11–26. (doi:10.1111/j.1365-2516.2008.01848.x)
2. Yuan H, Deng N, Zhang S, Cao Y, Wang Q, Liu X, Zhang Q. 2012 The unfolded von Willebrand factor response in bloodstream: the self-association perspective. *J. Hematol. Oncol.* **5**, 65. (doi:10.1186/1756-8722-5-65)
3. Cito S, Mazzeo MD, Badimon L. 2013 A review of macroscopic thrombus modeling methods. *Thromb. Res.* **131**, 116–124. (doi:10.1016/j.thromres.2012.11.020)
4. Huck V, Schneider MF, Gorzelanny C, Schneider SW. 2014 The various states of von Willebrand factor and their function in physiology and pathophysiology. *Thromb. Haemost.* **111**, 598–609. (doi:10.1160/TH13-09-0800)
5. Kim J, Zhang C, Zhang X, Springer TA. 2010 A mechanically stabilized receptor–ligand flex-bond important in the vasculature. *Nature* **466**, 992–995. (doi:10.1038/nature09295)
6. Ju L, Dong J, Cruz M, Zhu C. 2013 The N-terminal flanking region of the A1 domain regulates the force-dependent binding of von Willebrand factor to platelet glycoprotein Ibα. *J. Biol. Chem.* **288**, 32 289–32 301. (doi:10.1074/jbc.M113.504001)
7. Sing CE, Alexander-Katz A. 2011 Non-monotonic hydrodynamic lift force on highly-extended polymers near surfaces. *EPL* **95**, 48001. (doi:10.1209/0295-5075/95/48001)
8. Chen H, Fallah MA, Huck V, Angerer JI, Reininger AJ, Schneider SW, Schneider MF, Alexander-Katz A. 2013 Blood-clotting-inspired reversible polymer–colloid composite assembly in flow. *Nat. Commun.* **4**, 1333. (doi:10.1038/ncomms2326)
9. Huang J, Roth R, Heuser JE, Sadler JE. 2009 Integrin on human endothelial cells binds von Willebrand factor strings under fluid shear stress. *Blood* **113**, 1589–1597. (doi:10.1182/blood-2008-05-158584)
10. He G, Messina R, Hartmut L, Kiriy A. 2009 Shear-induced stretching of adsorbed polymer chains. *Soft Matter.* **5**, 3014–3017. (doi:10.1039/b906744b)
11. Chen H, Alexander-Katz A. 2013 Structure and dynamics of blood-clotting-inspired polymer-colloid composites. *Soft Matter.* **9**, 10 381–10 390. (doi:10.1039/c3sm52264d)
12. Sing CE, Alexander-Katz A. 2011 Equilibrium structure and dynamics of self-associating single polymers. *Macromolecules* **44**, 6962–6971. (doi:10.1021/ma200830t)
13. Sing CE, Alexander-Katz A. 2010 Elongational flow induces the unfolding of von Willebrand factor. *Biophys. J.* **98**, 35–37. (doi:10.1016/j.bpj.2010.01.032)
14. Alexander-Katz A, Netz RR. 2008 Dynamics and instabilities of collapsed polymers in shear flow. *Macromolecules* **41**, 3363–3374. (doi:10.1021/ma702331d)
15. Schneider SW, Nuschele S, Wixforth A, Gorzelanny C, Alexander-Katz A, Netz RR, Schneider MF. 2007 Shear-induced unfolding triggers adhesion of von Willebrand factor fibers. *Proc. Natl Acad. Sci. USA* **104**, 7899–7903. (doi:10.1073/pnas.0608422104)
16. Sing CE, Selvidge JG, Alexander-Katz A. 2013 Von Willlebrand adhesion to surfaces at high shear rates is controlled by long-lived bonds. *Biophys. J.* **105**, 1475–1481. (doi:10.1016/j.bpj.2013.08.006)
17. Alexander-Katz A. 2014 Toward novel polymer-based materials inspired in blood clotting. *Macromolecules* **47**, 1503–1513. (doi:10.1021/ma4007768)
18. Malevanets A, Kapral R. 1999 Mesoscopic model for solvent dynamics. *J. Chem. Phys.* **110**, 8605–8613. (doi:10.1063/1.478857)
19. Watari N, Makino M, Kikuchi N, Larson RG, Doi M. 2007 Simulation of DNA motion in a microchannel using stochastic rotation dynamics. *J. Chem. Phys.* **126**, 094902. (doi:10.1063/1.2538831)
20. Noguchi H, Gompper G. 2005 Dynamics of fluid vesicles in shear flow: effect of membrane viscosity and thermal fluctuations. *Phys. Rev. E* **72**, 011901. (doi:10.1103/PhysRevE.72.011901)
21. Chelakkot R, Winkler RG, Gompper G. 2012 Flow-induced helical coiling of semiflexible polymers in structured microchannels. *Phys. Rev. Lett.* **109**, 178101. (doi:10.1103/PhysRevLett.109.178101)
22. Ihle T, Kroll DM. 2001 Stochastic rotation dynamics: a Galilean-invariant mesoscopic model for fluid flow. *Phys. Rev. E* **63**, 020201. (doi:10.1103/PhysRevE.63.020201)
23. Alexander-Katz A, Schneider SW, Wixforth A, Netz RR. 2006 Shear-flow-induced unfolding of polymer globules. *Phys. Rev. Lett.* **97**, 138101. (doi:10.1103/PhysRevLett.97.138101)
24. Bell GL. 1978 Models for the specific adhesion of cells to cells. *Science* **200**, 618–627. (doi:10.1126/science.347575)
25. Siedieck CA, Lestini BJ, Kottke-Marchant KK, Eppell SJ, Wilson DL, Marchant RE. 1996 Shear-dependent changes in the three-dimensional structure of human von Willebrand factor. *Blood* **88**, 2939–2950.
26. Yago T *et al.* 2008 Platelet glycoprotein Ibα forms catch bonds with human WT vWF but not with type 2B von Willebrand disease vWF. *J. Clin. Invest.* **118**, 3195–3207.